

## Abstract

Multiwell assays based on the Boyden chamber have enabled highly parallel studies of chemotaxis (the directional migration of cells in response to molecular gradients), while direct-viewing approaches have allowed more detailed questions to be asked at low throughput. Boyden-based plates provide a count of cells that pass through a membrane, but no information about cell appearance. In contrast, direct viewing devices enable the observation of cells during chemotaxis, which allows measurement of many parameters including area, shape, and location. Here we show automated chemotaxis and cell morphology assays in a 96-unit direct-viewing plate. Using only 12,000 primary human neutrophils per datum, we measured dose-dependent stimulation and inhibition of chemotaxis and quantified the effects of inhibitors on cell area and elongation. With 60 parallel conditions and compatibility with existing lab automation, a dramatic increase in throughput compared to previously reported direct viewing approaches is achieved.

## Background

While modified Boyden chambers in multiwell format are the current standard for highly parallel studies of chemotaxis, direct-viewing approaches, where cells migrate on a horizontal surface, have particular advantages for quantitative studies, such as perturbation of function by drug candidates. The concentration profile experienced by cells in a Boyden chamber is unknown and may be influenced by cells as they traverse membrane pores. In contrast, the concentration gradient produced in direct-viewing devices can be verified using fluorescent dyes. Furthermore, the geometry of modified Boyden chambers is not conducive to microscopic study of cells during chemotaxis, which precludes the use of high content analysis. Existing direct-viewing methods tend to be complicated to run and challenged in terms of throughput. However, none of the direct-viewing approaches reported to date are suitable for highly parallel studies; the largest number of parallel conditions reported to date is twelve. The objective of our work was to develop a method that would provide the rich information of direct-viewing chemotaxis studies in an automated format with throughput comparable to Boyden-based plates. Automation allows highly parallel experiments to be run to study dose-dependent stimulation and inhibition of chemotaxis as well as chemoattractant and inhibitor effects on cell morphology.

## Direct Viewing Plate Supports Spontaneous Wick-Filling and Robust, Automated Cell Patterning

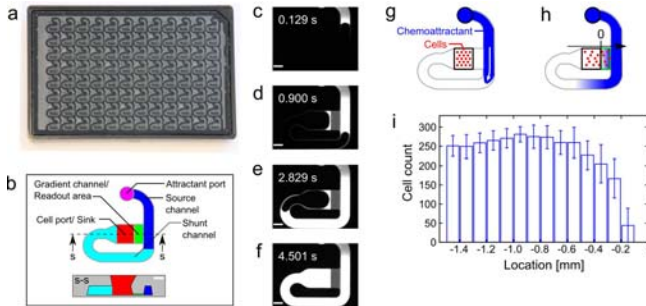


**Figure 1:** The iuvo™ Chemotaxis Assay Plate supports wick-filling and cell patterning. a) The plate (bottom view) has 96 microfluidic units. b) Each unit has five components: an attractant port and source channel where a chemoattractant is provided, a gradient channel connected to the source into which the chemoattractant diffuses to create a gradient, a sink (cell port) located at the other end of the gradient channel, and a shunt channel that helps sustain a stable gradient. "s-s" shows a cross-section along the dashed line. c-f) A time sequence showing wick-filling. g-h) A schematic representation of a chemotaxis assay. i) At the beginning of the assay the cells are distributed in a repeatable pattern in the cell port (N=13).

## Persistent Linear Gradients are Reproducibly Formed

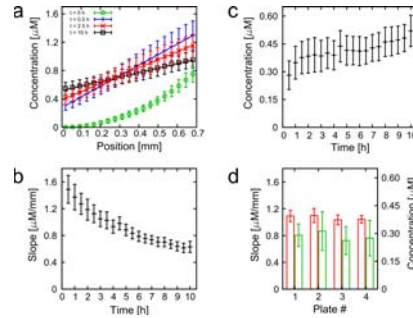


**Figure 2:** The iuvo™ Chemotaxis Assay Plate provides a repeatable linear gradient. a-d) Characterization of a molecular gradient (Alexa Fluor® 594) at 37°C. The graphs show a) gradient profile at 0, 0.5, 2.5 and 10 hours with best fit lines for the last three, b) the slope, and c) the concentration at the origin as determined by least squares line fit for each replicate. Graphs show mean values and standard deviations (N=13). d) The bar graph shows the slope (red) and concentration (green) at 2.5 hours in four different plates run at the same time.

## Effects of Chemoattractant and Inhibitors on Primary Neutrophil Chemotaxis

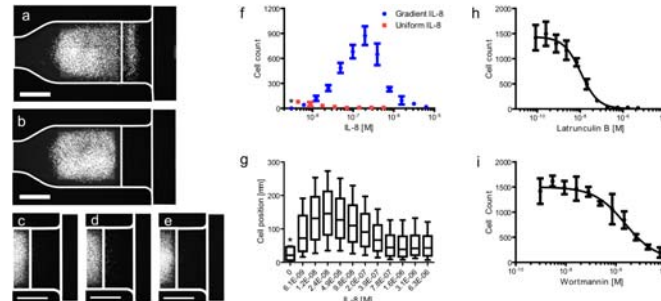


**Figure 3:** Dose-dependent stimulation and inhibition of chemotaxis. a-b) Cell distribution at the end of the assay after 2.5 hour incubation. a) 500 nM interleukin-8 (IL-8) gradient, b) no chemoattractant control. c-e) Cell migration in the presence of uniform IL-8 at c) 0.27 nM, d) 4.38 nM, and e) 560 nM. f) Dose dependent response to IL-8 gradients. The graph shows the mean and standard deviation for replicates of 4, except where indicated (\*\*\*) denotes replicate of 3). g) A box-whiskers plot (10%, 25%, 50%, 75%, 90%) indicating the distribution of cell positions at the assay endpoint as a function of IL-8 gradient source concentration. h-i) Dose-dependent inhibition of IL-8 mediated chemotaxis (500 nM source). Half-maximum inhibition concentrations ( $IC_{50}$ ) were found to be 10.8 nM for Latrunculin B and 2.32  $\mu$ M for Wortmannin. Preliminary assessment of data quality is encouraging for screening applications; Z=0.39 (data not shown).

## Effects of Chemoattractant on Myeloid Leukemia Cell Line Chemotaxis

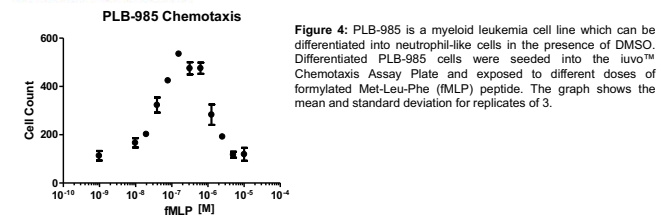


**Figure 4:** PLB-985 is a myeloid leukemia cell line which can be differentiated into neutrophil-like cells in the presence of DMSO. Differentiated PLB-985 cells were seeded into the iuvo™ Chemotaxis Assay Plate and exposed to different doses of formulated Met-Leu-Phe (fMLP) peptide. The graph shows the mean and standard deviation for replicates of 3.

## Morphological Analysis of Chemotactic Neutrophils

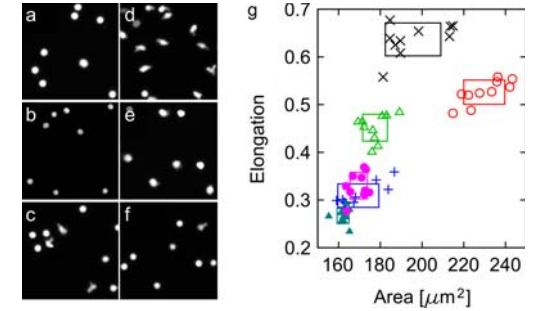


**Figure 5:** High content analysis of cell morphology reveals differential effects of inhibitors. Inhibition of neutrophil chemotaxis is associated with inhibitor-specific changes in area and elongation. For this experiment cells were seeded in the gradient channel prior to establishing gradient. Neutrophils were placed under experimental conditions with various concentration profiles of IL-8: a) none, b) uniform 0.4 nM, c) uniform 4 nM, or d-f) gradient with 62 nM source. The last condition was tested with d) no inhibitor, e) 10  $\mu$ M Wortmannin, and f) 1  $\mu$ M Latrunculin B. g) Scatter plot showing area and elongation. Each point represents one of ten replicates and the rectangles are centered at the mean and sized according to the mean  $\pm$  one standard deviation. Conditions shown are: control (+), uniform 0.4 nM IL-8 (dark green solid triangle), uniform 4 nM IL-8 (light green open triangle), 62 nM IL-8 gradient (X), gradient and 10  $\mu$ M Wortmannin (pink solid circle), gradient and 1  $\mu$ M Lat B (orange open circle), N=10 for each condition.

## Cell-Tracking in a Slide-Sized Device With Enclosure

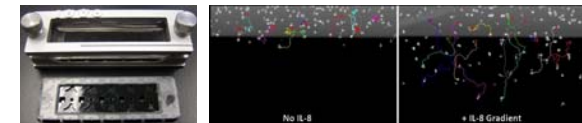


**Figure 6:** Live cell tracking in a slide-sized device with evaporation-preventing enclosure. Left panel: An aluminum frame with glass top and rubber gasket (top) was produced with standard 1" x 3" footprint to fit into slide holders and enable real-time live cell monitoring. Five individual chemotaxis units were prepared in each slide (bottom). Right panel: Neutrophil chemotaxis assay was hand pipetted using previously described conditions, with and without a gradient of 125 nM IL-8. Images were taken every minute over a 90 minute period in a temperature controlled environmental microscope chamber set to 37°C. Cell tracking software (Metamorph®, Molecular Devices) was used to quantify individual cell migration paths.

## Conclusions

- Microfluidic gradient channels arrayed in an SBS/ANSI standard plate were developed.
- The iuvo™ Chemotaxis Assay Plate enables robust delivery of reagents and cells using off-the-shelf lab automation hardware.
- Chemoattractant gradients are suitable for quantification of polymorphonuclear leukocyte chemotaxis.
- $IC_{50}$  values of dose response to migration inhibitors was demonstrated.
- Migration on a horizontal surface enables high content analysis such as shape and area.
- Effects of compounds on cell morphology can be quantified to distinguish different classes of inhibitors.

## Acknowledgements

The authors thank Anna Huttenlocher at University of Wisconsin-Madison for assistance with protocols and cells. Funding for this work was provided by NIH grant # 2 R44 HL088785-02. United States Patent Application 20090123961.